



Fermi
Gamma-ray Space Telescope



Search for dark matter-related features in the Galactic gamma-ray energy spectra

Francesco Loparco
(francesco.loparco@ba.infn.it)

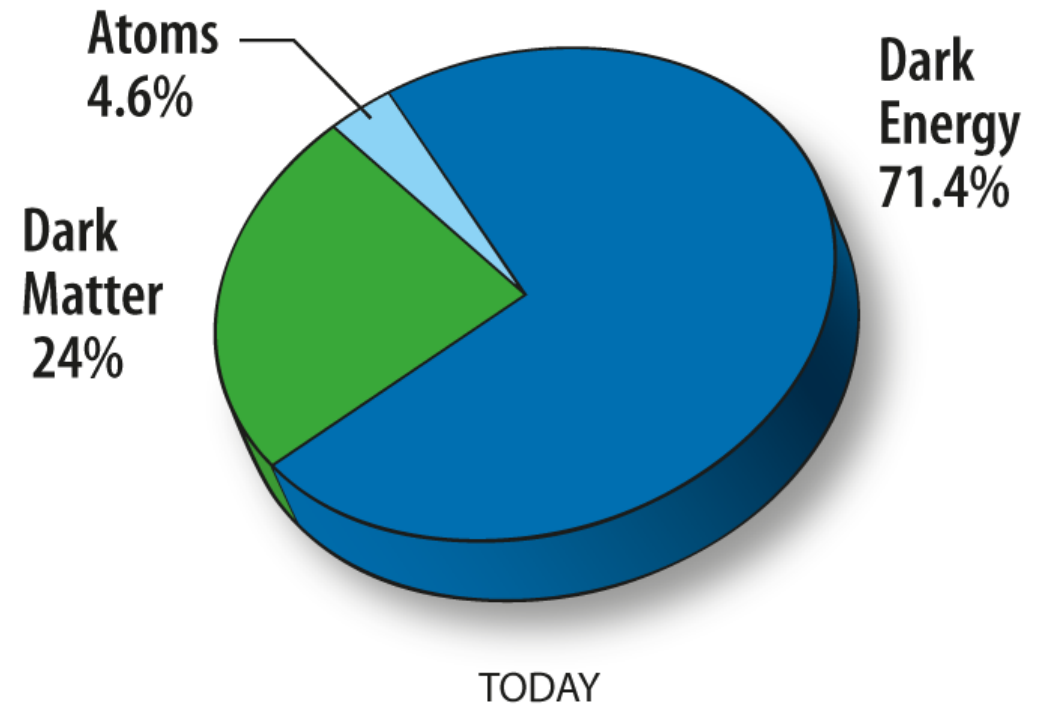
Mario Giliberti

Nicola Mazziotta

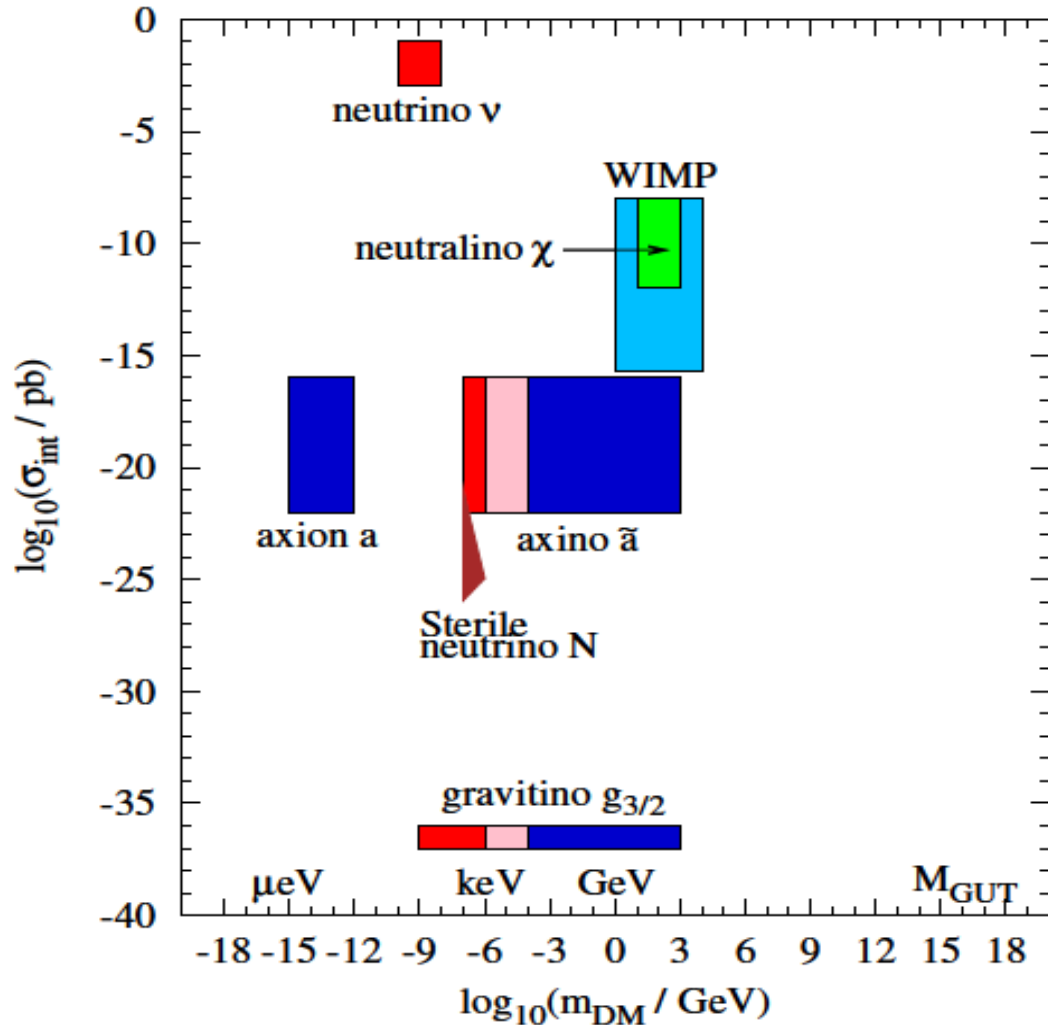
on behalf of the Fermi-LAT Collaboration

Dark Matter (DM)

- **Astrophysical evidence for missing mass**
 - Galaxy rotation curves
 - Dynamics of galaxy clusters
 - Gravitational lensing of galaxy clusters
 - Collisions of galaxy clusters
 - Cosmological probes
- **Observational evidence indicates that:**
 - DM is non-baryonic
 - DM (almost totally) neutral
 - DM (almost totally) collisionless
 - DM is stable (decay times >13 Gyrs)
 - DM is cold (non-relativistic)



Possible DM candidates

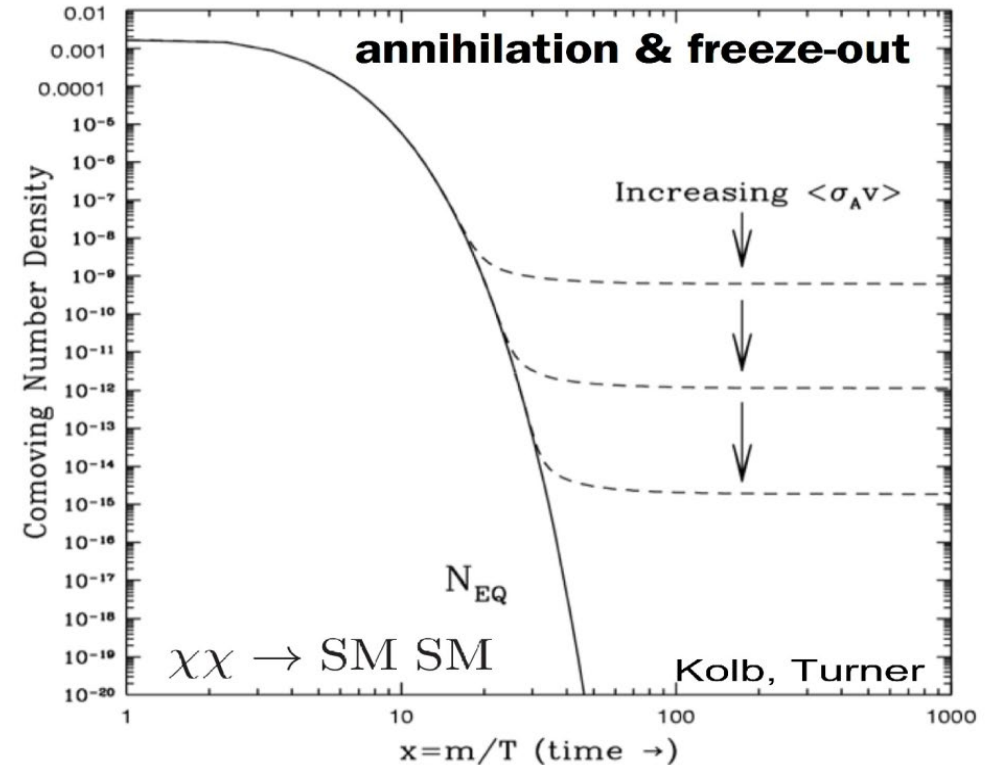


- DM candidates include a large number of particles, covering a wide range of masses
- The cross sections for DM interactions with ordinary matter also cover a wide range and are strongly motivated by particle physics

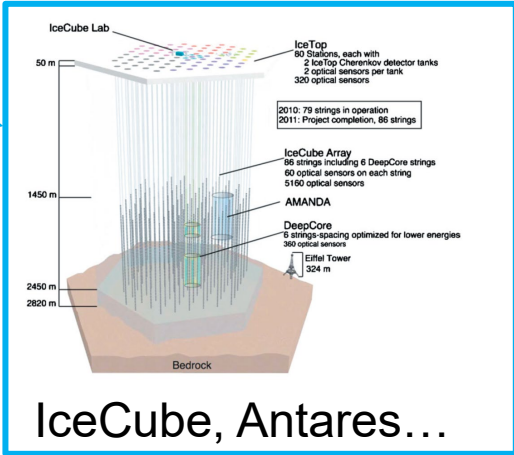
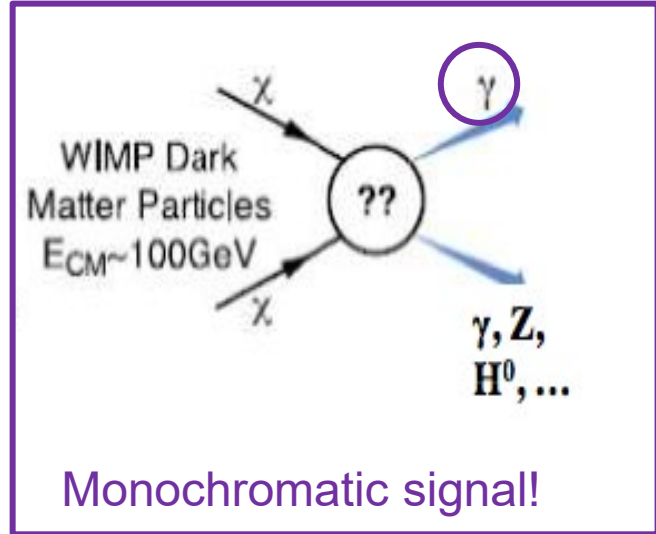
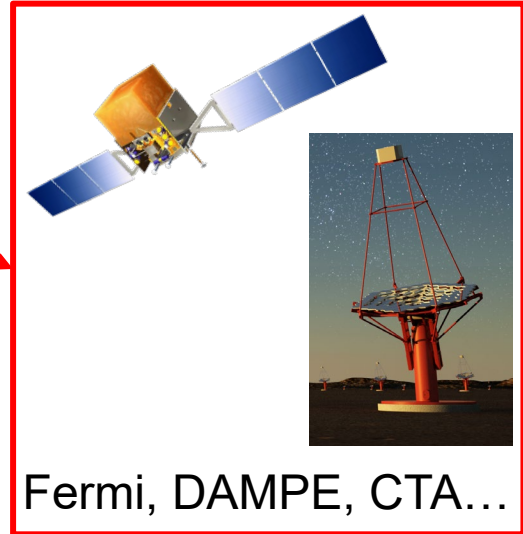
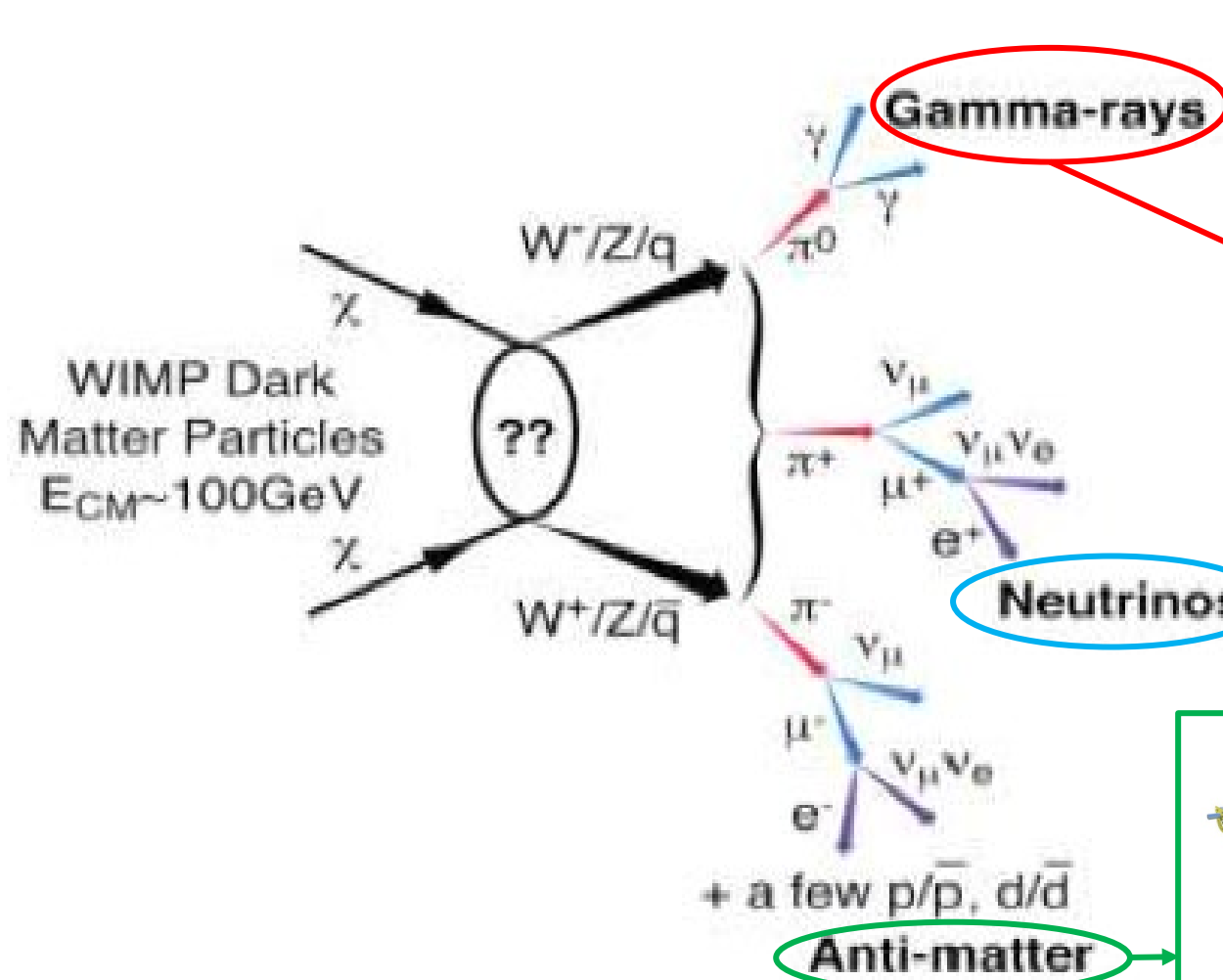
Plot taken from Roszkowski et al., Rep. Prog. Phys. 81 (2018), 6, arXiv 1707.06277

WIMPs as DM candidates

- A WIMP in chemical equilibrium in the early universe naturally has the right density to be cold Dark Matter
 - At early times, WIMPs are produced in $I+I$, ... collisions in the hot primordial soup (thermal production)
 - WIMP production ceases when the production rate becomes smaller than the Hubble expansion rate (freeze-out)
 - After freeze-out, the number of WIMPs per photon is constant
- Standard relic density calculation yields for nonrelativistic relics:
 - $\Omega_{dm} h^2 \approx \frac{3 \times 10^{-27} \text{ cm}^3 \text{ s}^{-1}}{\langle \sigma v \rangle} \approx 0.1$
- Electroweak cross-sections are in correct range:
 - $\langle \sigma v \rangle \sim 10^{-26} \text{ cm}^3 \text{ s}^{-1}$

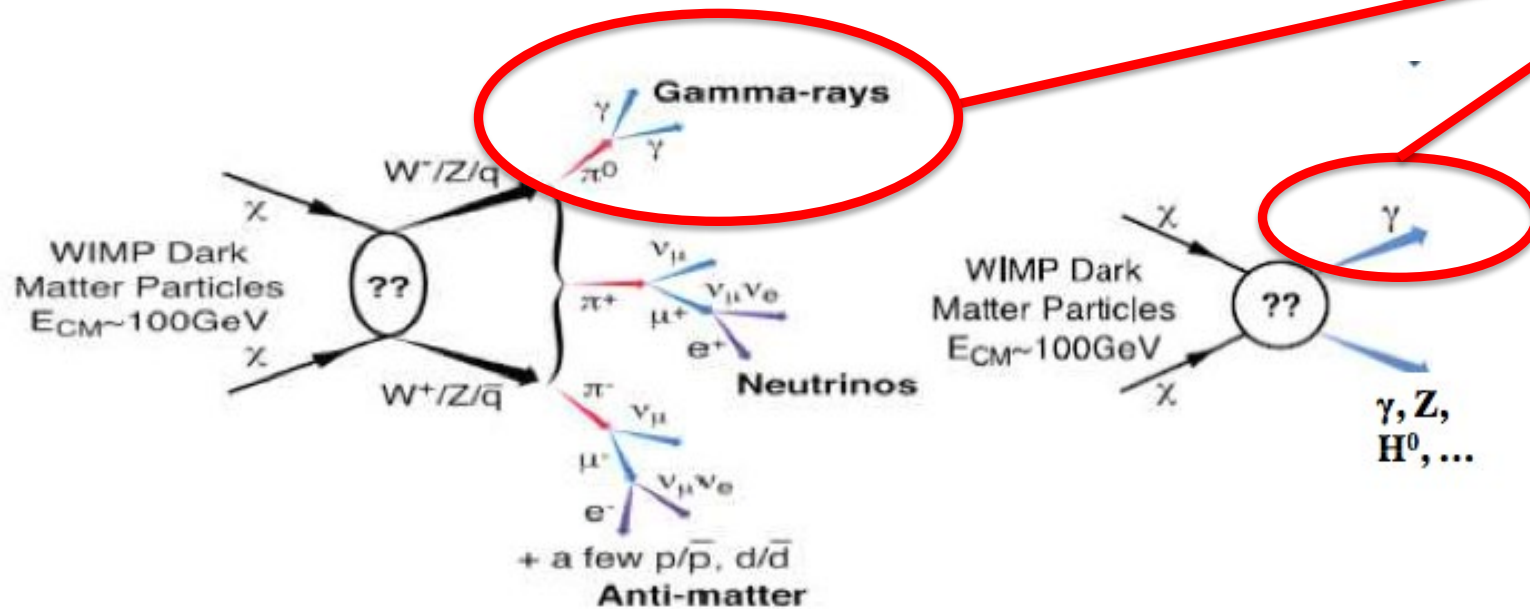
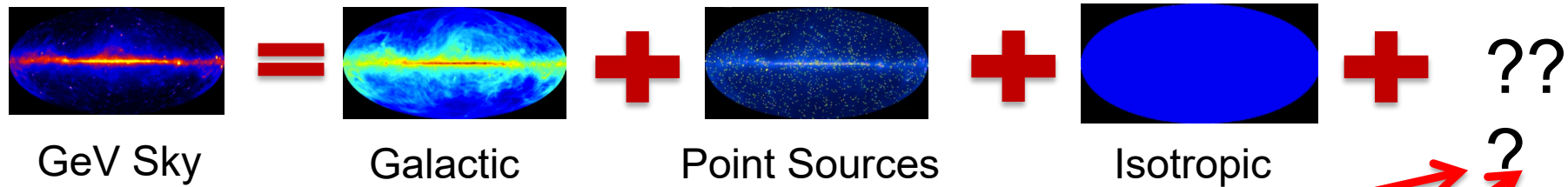


Indirect DM searches



Indirect searches with gamma rays

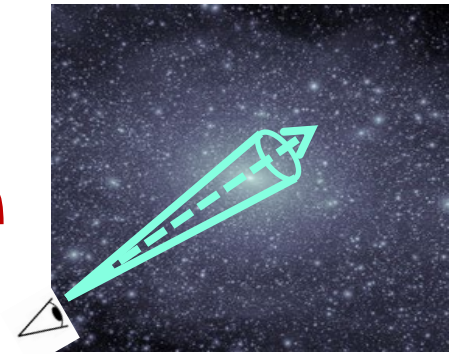
- Indirect detection (i.e. astrophysical) searches for DM in the astrophysical targets where it is known to exist



Gamma-ray flux from DM annihilations/decays

Observed flux Intrinsic Particle Properties Astrophysics

$$\phi(E, \Delta\Omega) = \frac{1}{4\pi} \frac{\langle\sigma v\rangle}{2 m_\chi^2} \sum_f \frac{dN_f}{dE} B_f \int_{\Delta\Omega} d\Omega \int_{\text{l.o.s.}} dl \rho^2(l(\Omega))$$



Annihilation:

$\langle\sigma v\rangle \sim 3 \times 10^{-26} \text{ cm}^3/\text{s}$
for thermal relic

J-factor: originates from the DM distribution (line-of-sight integral)

Decay:

$$\phi(E, \Delta\Omega) = \frac{1}{4\pi} \frac{1}{\tau m_\chi} \sum_f \frac{dN_f}{dE} B_f \int_{\Delta\Omega} d\Omega \int_{\text{l.o.s.}} dl \rho(l(\Omega))$$

The Fermi Gamma-ray Space Telescope

- The Fermi Gamma-Ray Space Telescope (FGST) is an international space mission to study astrophysical gamma rays
- The satellite is equipped with two main instruments:
 - **Gamma-Ray Burst Monitor (GBM)**
 - **Energy range from 8keV to 40MeV**
 - **Large Area Telescope (LAT)**
 - **Energy range from 20MeV to >300GeV**
- The satellite was launched on June, 11th 2008 from the Cape Canaveral Air Force Station (Florida)
- Fermi is on a nearly circular orbit
 - **Altitude = 565 km at launch (now 537 km)**
 - **Inclination = 25.6°**
 - **Period = 96 minutes**
- **Mission extended until 2025 after the NASA Senior Review in 2022**

The Fermi LAT

Precision Si-strip Tracker (TKR)

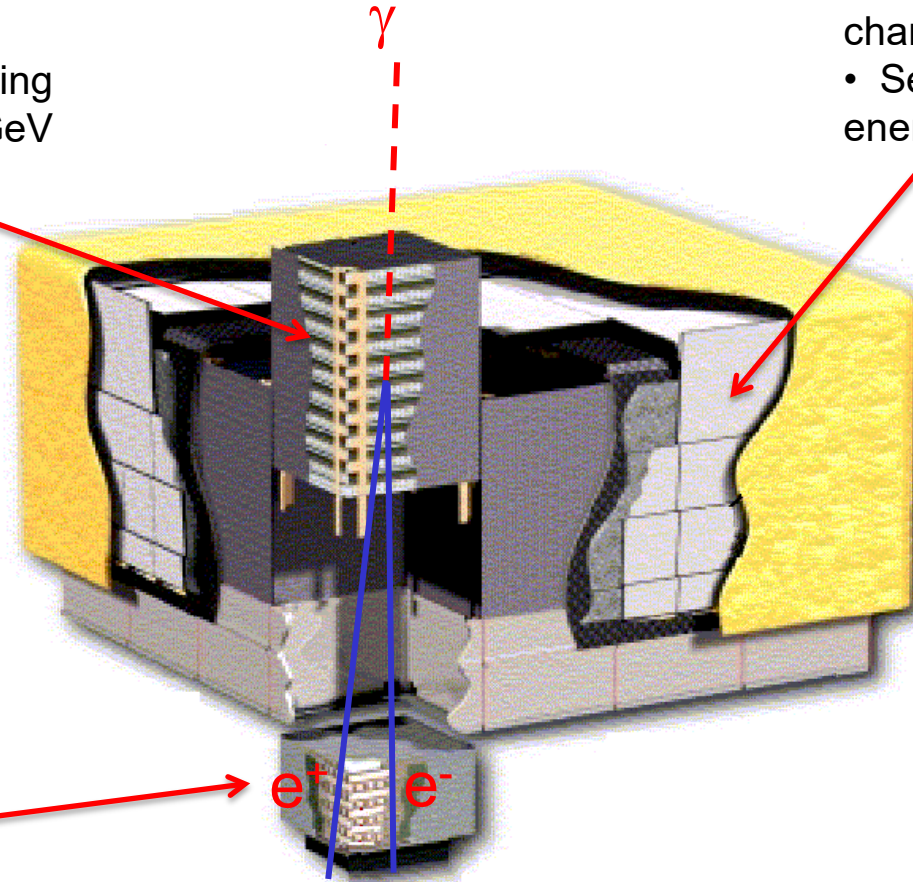
- Measures incident γ -ray direction
- 18 XY tracking planes: 228 μm strip pitch
- High efficiency. Good position resolution
- 12x 0.03 X_0 front end \rightarrow reduce multiple scattering
- 4x 0.18 X_0 back-end \rightarrow increase sensitivity >1 GeV

Anticoincidence Detector (ACD)

- 89 scintillator tiles
- First step in the reduction of large charged cosmic ray background
- Segmentation reduces self-veto at high energy

Hodoscopic CsI Calorimeter

- Segmented array of 1536 CsI(Tl) crystals
- 8.6 X_0 : shower max contained
 ~ 200 GeV normal (1.5 X_0 from TKR included)
 $\sim 1\text{TeV}$ @ 40° (CAL-only)
- Measures the incident γ -ray energy
- Rejects cosmic-ray background



Electronics system

- Includes flexible, highly efficient, multi-level trigger

The LAT instrument response functions (IRFs)

- The expected count rate from a given source can be expressed as:

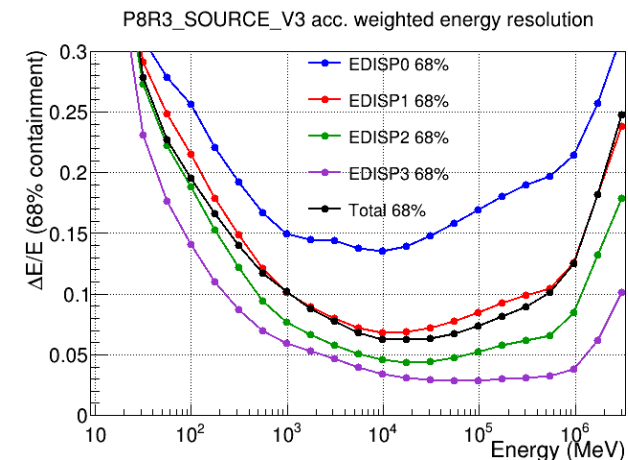
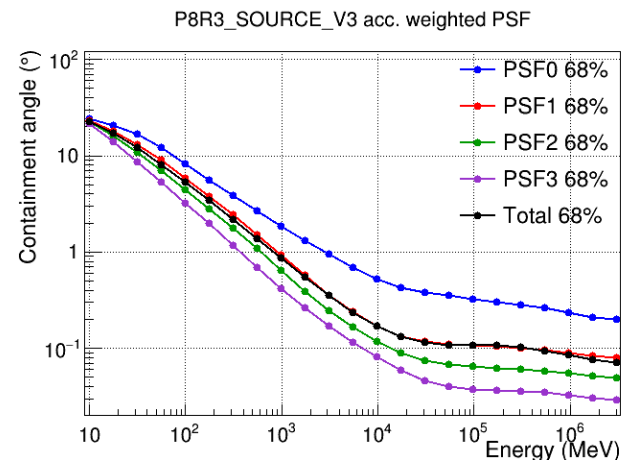
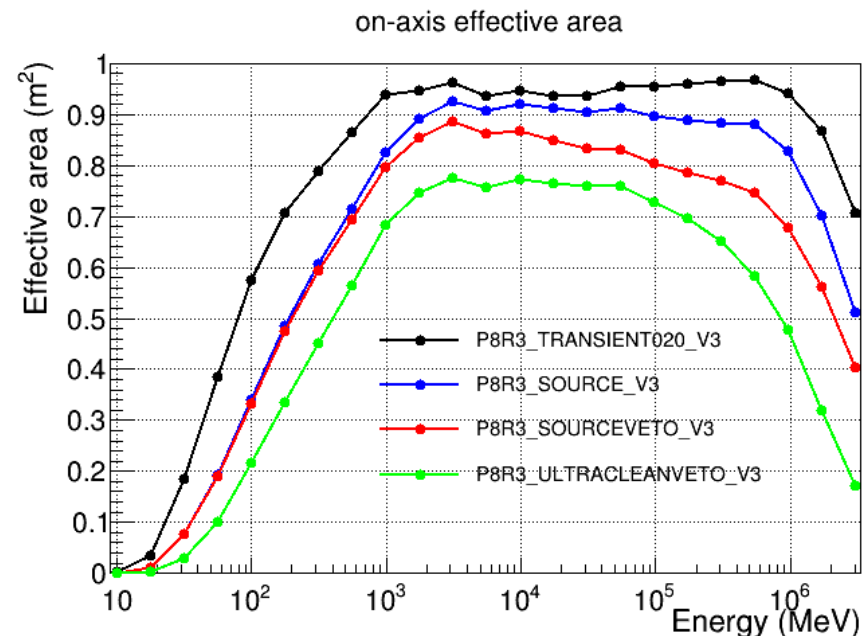
$$r(E', \hat{\nu}') = \iint dE d\hat{\nu} R(E', \hat{\nu}', E, \hat{\nu}) \Phi(E, \hat{\nu})$$

- $E', \hat{\nu}'$ = measured photon energy and arrival direction
 - $E, \hat{\nu}$ = true photon energy and arrival direction
 - $\Phi(E, \hat{\nu})$ = photon flux from the source
 - $R(E', \hat{\nu}', E, \hat{\nu})$ = instrument response function (IRF)
- The IRF can be factorized as:

$$R(E', \hat{\nu}', E, \hat{\nu}) = A_{eff}(E, \hat{\nu}) P(\hat{\nu}', E, \hat{\nu}) D(E', E, \hat{\nu})$$
 - $A_{eff}(E, \hat{\nu})$ = effective area
 - A_{eff} is the cross section of the LAT for detecting a photon with true energy E coming from the direction $\hat{\nu}$
 - $P(\hat{\nu}', E, \hat{\nu})$ is the point spread function (PSF)
 - The PSF is the probability that a photon with true energy E coming from the direction $\hat{\nu}$ is observed as coming from $\hat{\nu}'$
 - $D(E', E, \hat{\nu})$ is the energy dispersion
 - The energy dispersion is the probability that a photon with true energy E coming from the direction $\hat{\nu}$ is observed with energy E'

The LAT instrument response functions (IRFs)

- Events are subdivided into classes
 - Each class is characterized by its own set of IRFs
- Classes are nested hierarchically
 - Higher probability photon selections have smaller effective areas, narrower PSFs and lower background contamination
- Events within each class are subdivided into event types
 - **PSF event types:** based on the quality of the reconstructed direction, the data are divided into quartiles, from the worst quality quartile (PSF0) to the best quality quartile (PSF3)
 - **EDISP event types:** based on the quality of the energy reconstruction, from the worst quality quartile (EDISP0) to the best quality quartile (EDISP3)



DM searches with gamma rays from the Milky Way Halo

- Our Galaxy is an excellent target for dark matter (DM) searches with gamma rays
 - The disk of the Milky Way is thought to be embedded in a much larger, roughly spherical, DM halo
- **Direct production:** WIMPs in the Milky Way halo can annihilate ($\chi\chi \rightarrow \gamma\gamma$) or decay ($\chi \rightarrow \gamma\gamma$) into gamma rays
 - Both processes yield monochromatic photons
 - Line-like features expected in the Galactic gamma-ray spectra
 - Line searches already performed by the Fermi-LAT Collaboration with null results
 - Further details in M. Ackermann+, PRDD91 (2015), 122002 and references therein
 - Claim of a possible line feature at 133 GeV in 2012 (Bringmann+, JCAP 07, 054, Weniger+, JCAP 08, 007)
 - The feature turned out to be insignificant
- **Indirect production:** WIMPs in the halo can annihilate ($\chi\chi \rightarrow \phi\phi$) or decay ($\chi \rightarrow \phi\phi$) into light mediators, which in turn decay into pairs of photons ($\phi \rightarrow \gamma\gamma$)
 - Box-like features expected in the Galactic gamma-ray spectra

- WIMP annihilations in the Galactic Halo may yield gamma rays through the annihilation process:

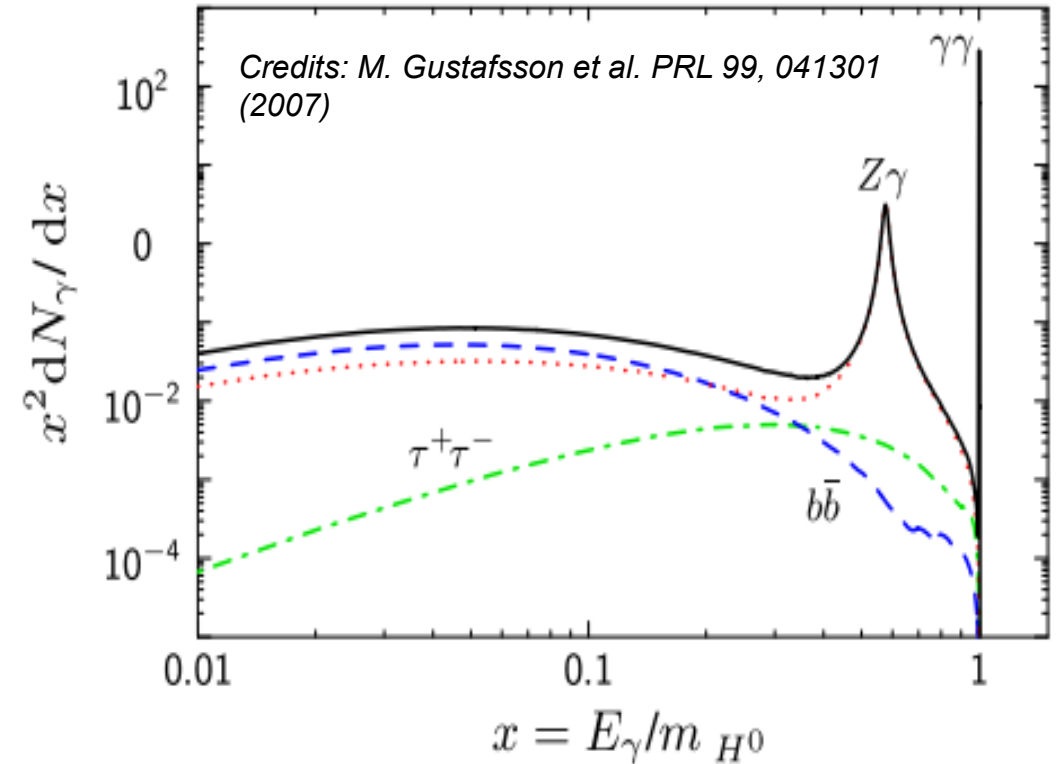


with $X = \gamma, Z^0, H^0$

- If the two DM particles annihilate at rest, the gamma-ray energy will be

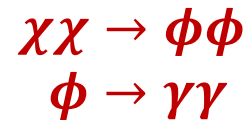
$$E_\gamma = m_\chi - \frac{m_X^2}{4m_\chi}$$

- If X is another photon, then $E_\gamma = m_\chi$
- Sharp, distinct spectral feature (“smoking gun”)
 - Likely a small branching fraction ($\sim 10^{-2}$ to 10^{-4})
 - Signal predicted to be small
- In case of decay $\chi \rightarrow \gamma + X$ the photon energy is obtained from the previous formula with the substitution $m_\chi \rightarrow m_\chi/2$



Box-like features in the gamma-ray spectra from DM

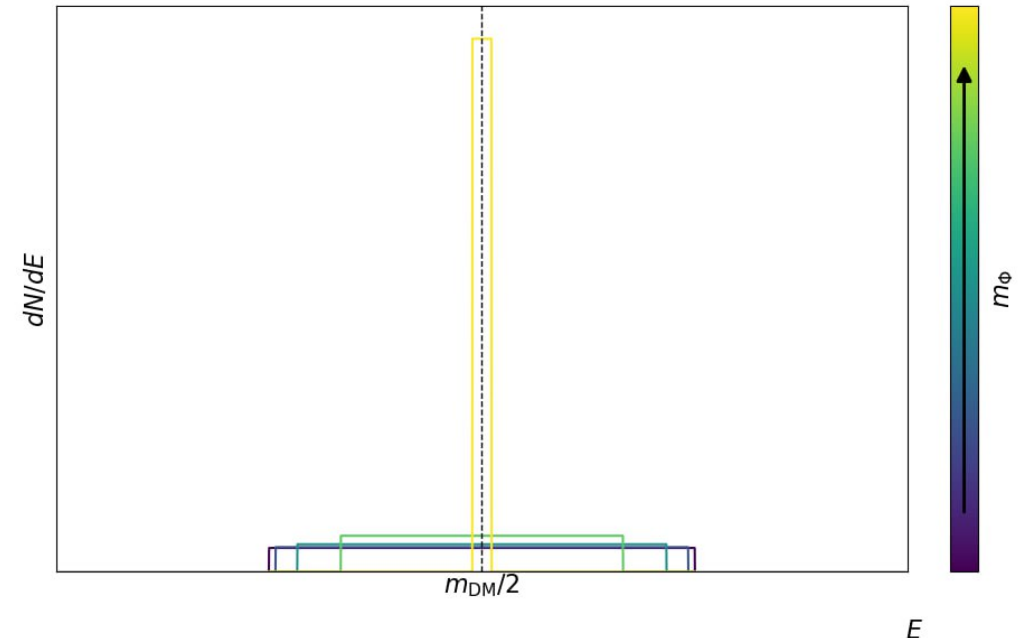
- DM particles in the Milky Way Halo could annihilate into pairs of long-lived mediators that would then decay into gamma rays after traveling in the Galaxy:



- A box-shaped gamma-ray spectrum is expected
- For light mediators ($m_\phi \ll m_\chi$) the box lower edge is found at $E_\gamma = 0$, while the upper edge is found at $E_\gamma = m_\chi$
 - In this case:

$$\frac{dN_\gamma}{dE} = 2H(E_{box} - E)$$

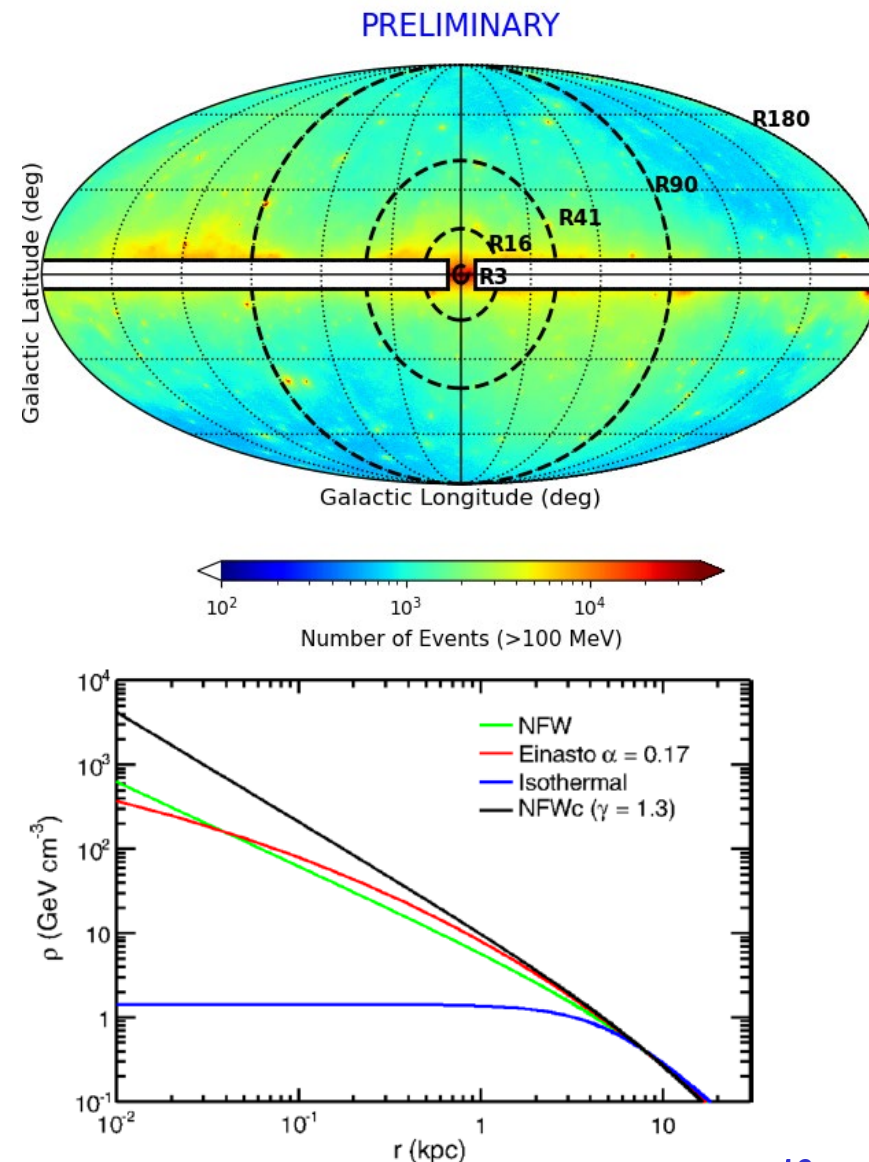
- E_{box} is the upper edge of the box
- in the limit $m_\phi \rightarrow m_\chi$ the box-like feature reduces to a line-like feature at $E_\gamma = m_\chi/2$



- **Observation time: August 2008 – December 2023 (15.5 years)**
- **Energy Range: 100 MeV – 2 TeV**
- **Zenith angle: $\vartheta_{zen} < 100^\circ$**
- **Event class: CLEAN**
- **Event type: all event types**
 - **The event sample is partitioned in 4 subsamples, according to the LAT energy resolution (from EDISP0 worst, to EDISP3 best)**
 - **Different analyses performed for each EDISP sample**
 - **Combined analysis of all EDISP samples**
- **Data Quality:**
 - **DATA_QUAL==1**
 - **LAT_CONFIG==1**
 - **IN_SAA!=T**

Regions of Interest (Rols)

- We follow the approach in the previous LAT papers
 - See Ackermann+, PRD91, 122002 (2015)
- We select 5 different Regions of Interest (Rols) corresponding to cones with the axis pointing towards the Galactic Center (GC), with different angular radii:
 - R3 (3°): optimized for NFWc DM density profile
 - R16 (16°): optimized for Einasto DM density profile
 - R41 (41°): optimized for NFW DM density profile
 - R90 (90°): optimized for Isothermal DM density profile
 - R180 (whole sky): optimized for decay searches only, NFW profile
- A mask, corresponding to the region $|b| < 5^\circ$ $|l| > 6^\circ$ (Galactic Plane, GP) is applied to all ROIs (with the exception of R3)
- The GP is used as control region



Flux models

- Flux in the ROI: $\phi_{ROI}(E) = \phi_{sig}(E) + \phi_{ROI,bkg}(E)$
- Flux in the control region (GP): $\phi_{GP}(E) = \phi_{GP,bkg}(E)$
- The signal flux is modeled either as a **line** ($\phi_{sig}(E) = s\delta(E - E_{fit})$) or as a **box** ($\phi_{sig}(E) = s\Theta(E - E_{fit})$)
 - In both cases only one fit parameter ($s > 0$, corresponding to the intensity of the feature)
- The background flux is modeled as the sum of a smooth component and a possible feature with the same shape as the signal:

$$\phi_{ROI,bkg}(E) = \phi_{ROI,smooth}(E) + \phi_{bkg,feature}(E)$$

$$\phi_{GP,bkg}(E) = \phi_{GP,smooth}(E) + \phi_{bkg,feature}(E)$$

- The smooth component is modeled either as a log-parabola or as a power-law:

$$\phi_{smooth}(E) = \begin{cases} k \left(\frac{E}{E_0}\right)^{-\Gamma - \beta \log\left(\frac{E}{E_0}\right)} & \text{if } E_{fit} < 10\text{GeV} \\ k \left(\frac{E}{E_0}\right)^{-\Gamma} & \text{if } E_{fit} > 10\text{GeV} \end{cases}$$

- Different smooth components in the ROI and in the GP → Up to 6 fit parameters ($k_{ROI}, \Gamma_{ROI}, \beta_{ROI}, k_{GP}, \Gamma_{GP}, \beta_{GP}$)
- The feature component is either a **line** ($\phi_{bkg,feature}(E) = b\delta(E - E_{fit})$) or as a **box** ($\phi_{bkg,feature}(E) = b\Theta(E - E_{fit})$)
 - The feature component is the same in the ROI and in the control region → Only 1 fit parameter (b)

Likelihood analysis

- For each ROI and for each EDISP event sub-sample, a maximum likelihood analysis in sliding energy windows has been implemented
 - Fit energy range from 1 GeV to 1 TeV
- Given the fit energy E_{fit} , the associated window is the interval $[E_{fit}(1 - w), E_{fit}(1 + w)]$
 - Analysis performed with $w = 0.40, 0.50, 0.60$
 - The center of the window corresponds to the line energy or to the upper edge of the box
- The log-likelihood ratio is defined as:

$$\log \lambda(\vec{\theta}) = \log \left[\mathcal{L}(\vec{n} | \vec{\mu}(\vec{\theta})) / \mathcal{L}(\vec{n} | \vec{n}) \right] = \sum_j [-(\mu_j + n_j) + n_j \log(\mu_j / n_j)]$$

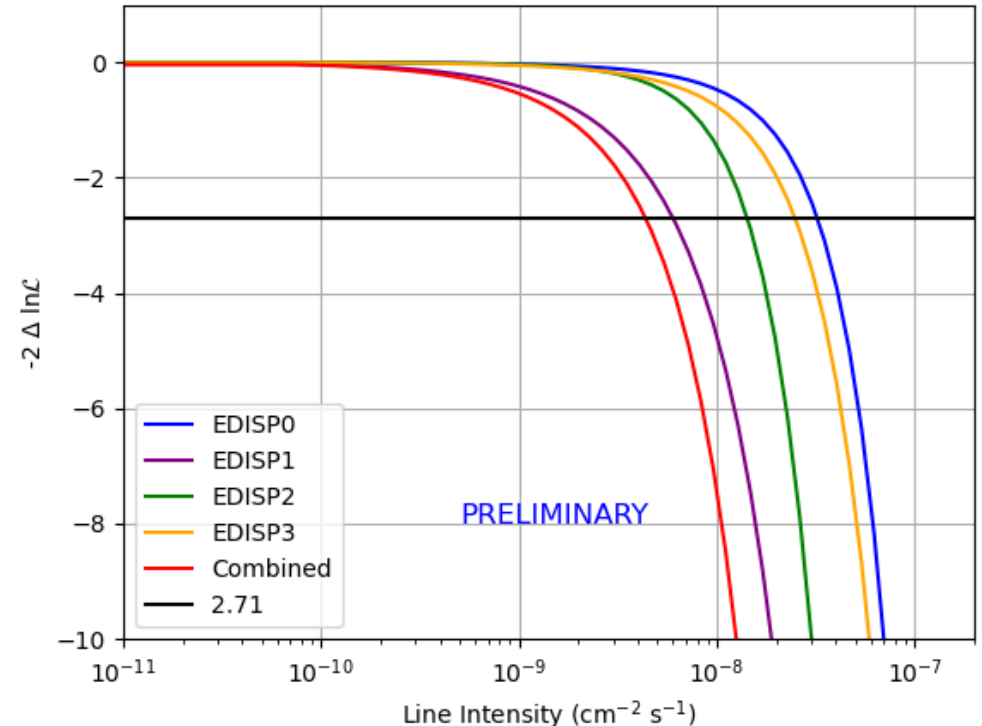
- $\vec{n} = (n_1, n_2 \dots)$ and $\vec{\mu} = (\mu_1, \mu_2 \dots)$ are the vectors of observed and expected counts
 - Expected counts are evaluated folding the flux models with the exposures
- $\vec{\theta} = (k_{ROI}, \Gamma_{ROI}, \beta_{ROI}, k_{GP}, \Gamma_{GP}, \beta_{GP}, b, s)$ is the vector of the fit parameters
 - The strength of the signal feature s is allowed to take only positive values
 - The null hypothesis (no signal) is obtained when $s = 0$
 - The strength of the background feature b can take either positive or negative values
- The parameters $\vec{\theta}_{max}$ which maximize the likelihood are obtained from a MINUIT fit
- We also combine the log-likelihood ratios of all EDISP sub-samples:

$$\log \lambda_{comb}(s) = \sum_i \log \lambda_i(s)$$

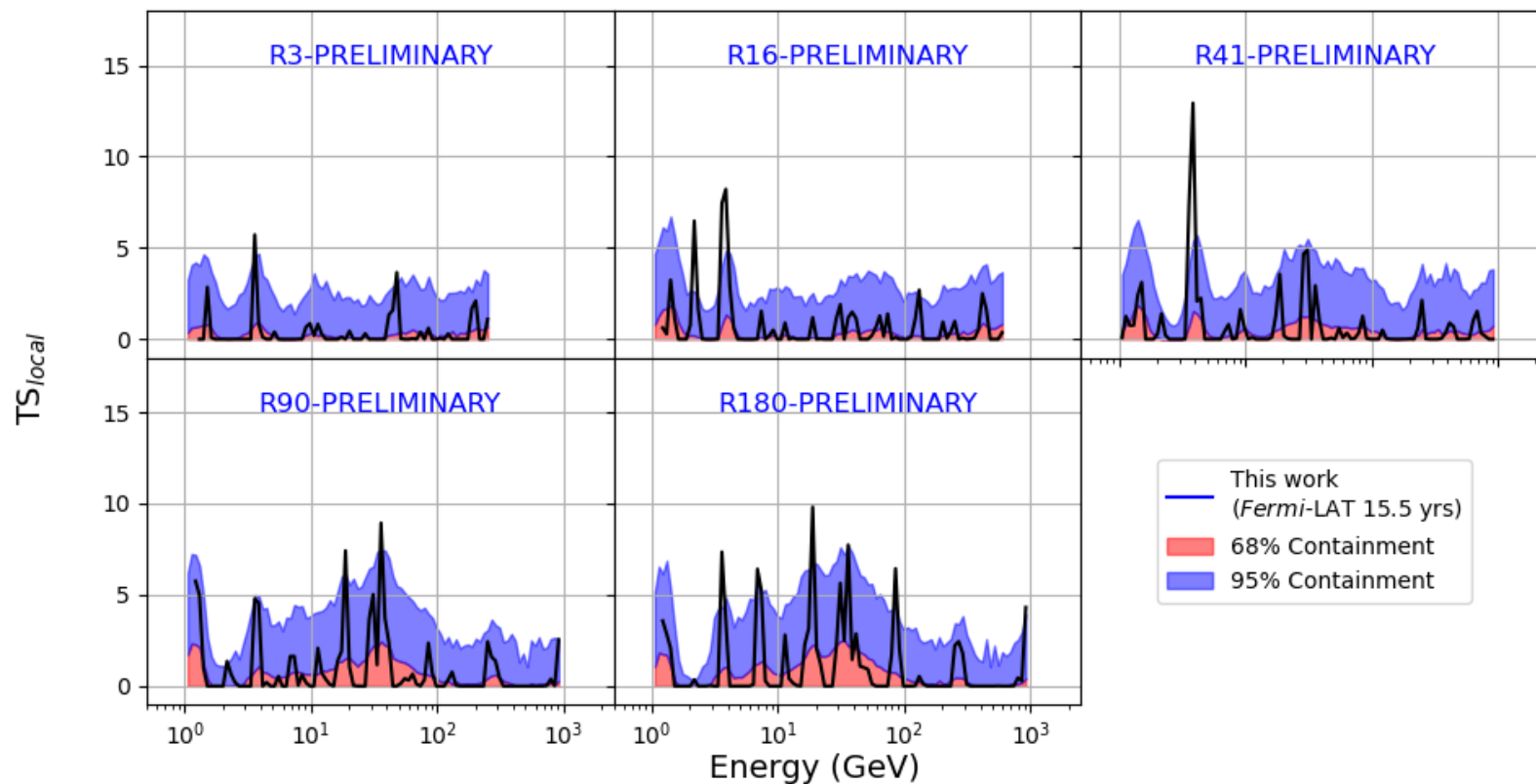
Hypothesis test

- The background parameters are fixed to the fitted values :
 - $\vec{\theta}_b = \vec{\theta}_{b,max} \equiv (k_{ROI,max}, \Gamma_{ROI,max}, \beta_{ROI,max}, k_{GP,max}, \Gamma_{GP,max}, \beta_{GP,max}, b_{max})$
- We evaluate the log-likelihood ratio for the null hypothesis ($s = 0$) and for the alternative hypothesis:
 - $\log \lambda_0 = \log \lambda(\vec{\theta}_{b,max}, s = 0)$
 - $\log \lambda_1 = \log \lambda(\vec{\theta}_{b,max}, s)$
- Test statistics of the fit (local):

$$TS = 2[\log \lambda_{1,max} - \log \lambda_0]$$
 - TS is expected to obey a χ^2 distribution with 1 d.o.f.
 - The local significance level of the feature (in σ units) is given by \sqrt{TS}
 - A feature is significantly detected if $TS > 25$
- Upper limits (ULs) on the signal strength s are calculated by studying the variations of TS as a function of s
 - The UL on s at 95% confidence level (CL) is obtained by setting $TS = TS_{min} + 2.71$



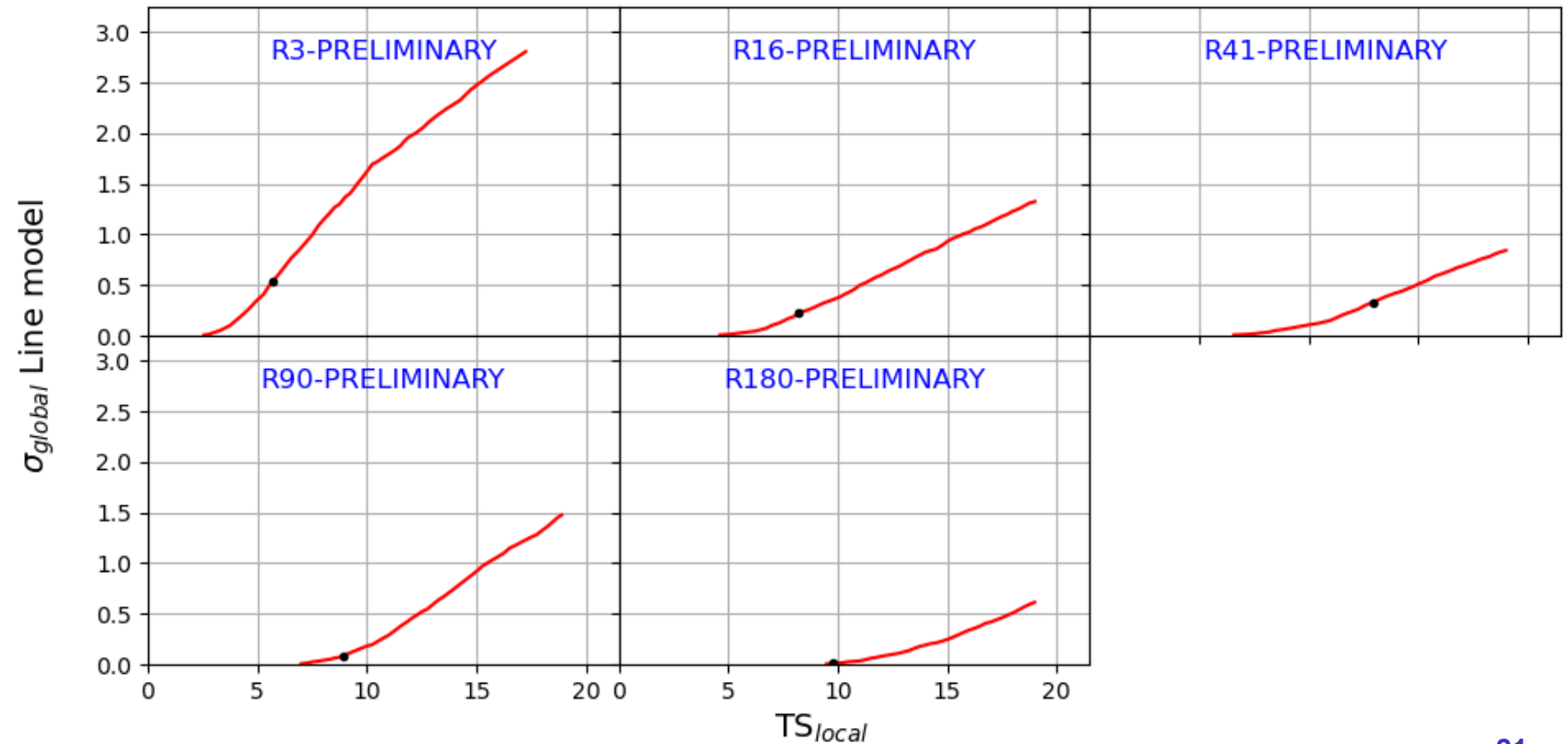
Results for the line searches: local significance of possible features



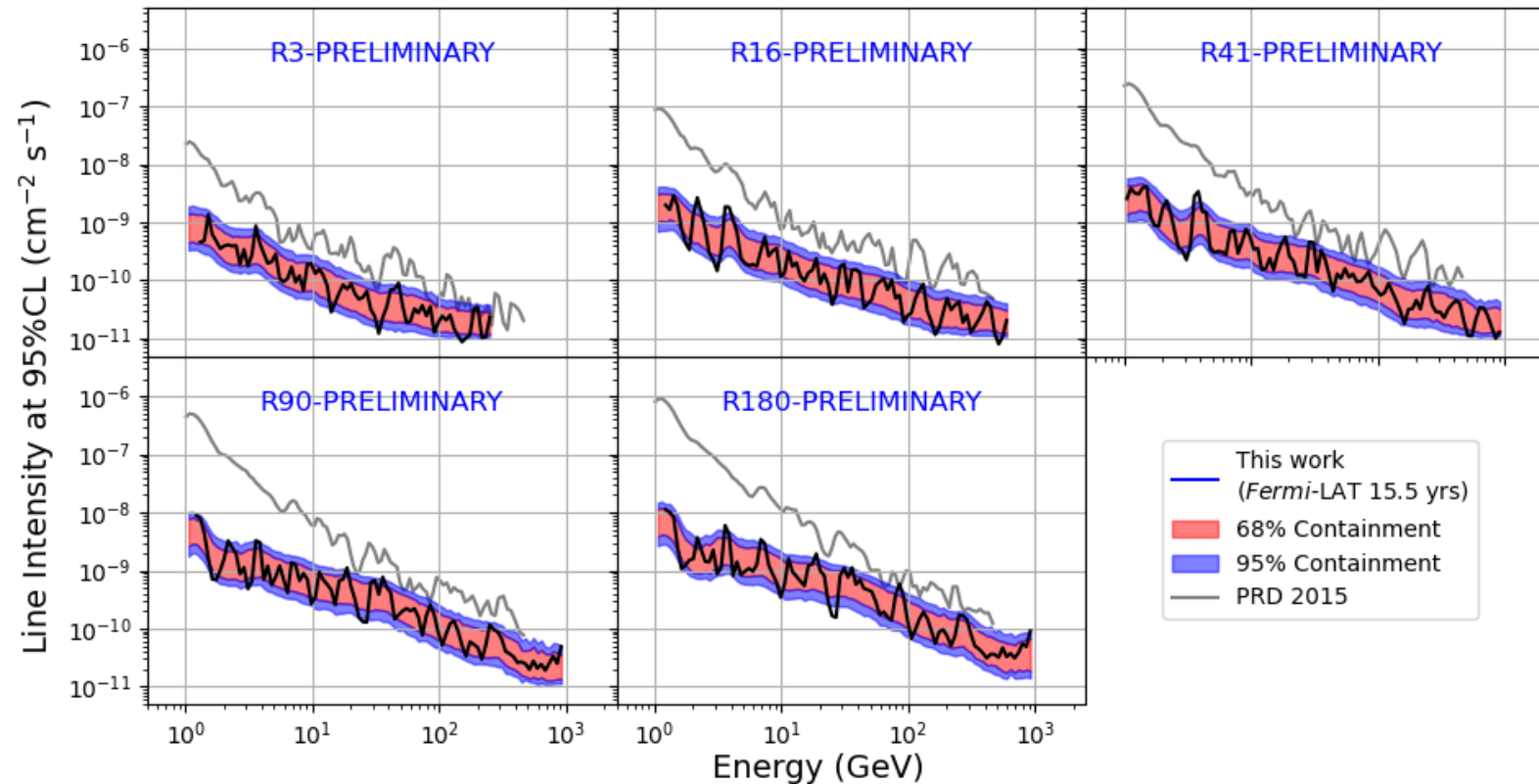
- 1000 background-only simulated pseudo-experiments:
 - Counts in each energy bin extracted from a Poisson distribution with its average value taken from a template model (null hypothesis)
 - Same analysis chain as real data
 - ULs at 95% and TS distributions are evaluated
 - From the quantiles of the distributions 68% (red) and 95% (blue) containment bands are built
- Results consistent with expectations from the null hypothesis, with few outliers

Global significance

- From the pseudo-experiments we build the distribution of the maximum local TS and we evaluate its quantiles
 - Assuming that the global significance obeys a half-normal distribution, we associate a global significance to each value of TS
 - The quantiles are converted in σ units
- All features are globally insignificant
- In our data the potential feature with the highest global significance is found in R3, but its global significance is $\sim 0.55\sigma$



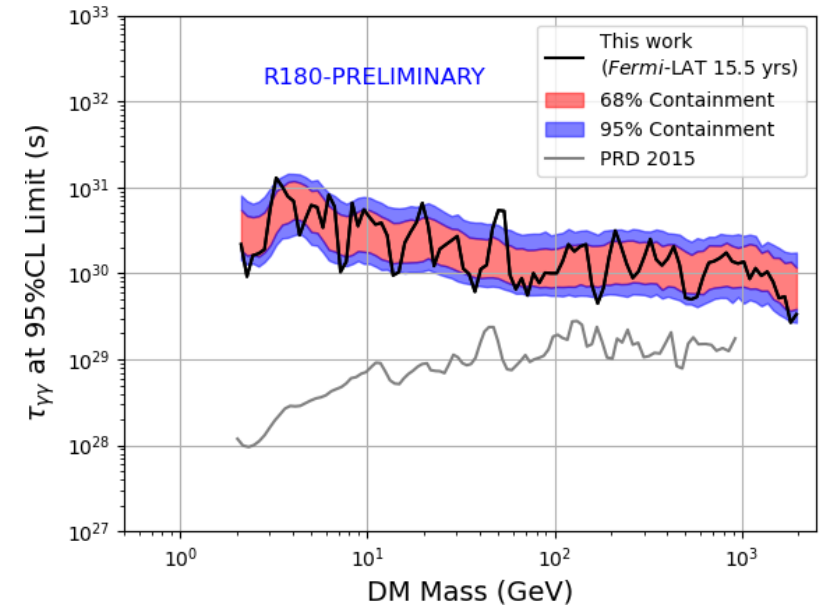
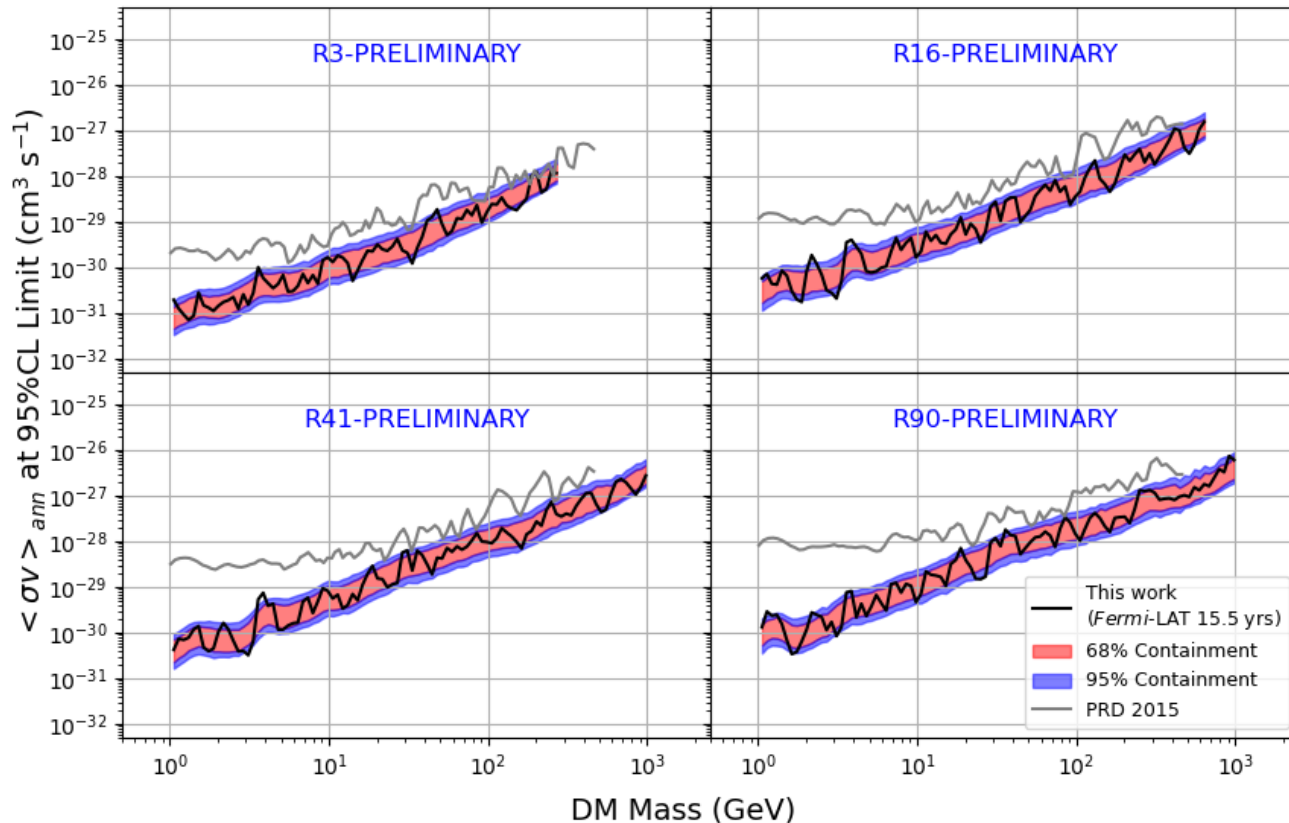
Results for the line searches: upper limits on the line intensity



- Measured limits lie within the containment bands, and are therefore consistent with the expectations for the null hypothesis
- Constraints on the line intensity up to 2 orders of magnitude stronger than those obtained in 2015

Constraints on $\langle\sigma v\rangle$ and τ from line search

- Upper limits on signal strength converted into physical parameters of interest $\langle\sigma_{ann}v\rangle$ and $\tau_{\gamma\gamma}$
 - The upper limits on $\langle\sigma_{ann}v\rangle$ lie in the interval $10^{-30} - 10^{-26} \text{ cm}^3 \text{ s}^{-1}$
 - The lower limits on $\tau_{\gamma\gamma}$ are in the range $10^{30} - 10^{31} \text{ s}$
- Constraints up to a factor 100 stronger than those obtained in 2015



- **We implemented dedicated algorithm to search for possible features in the gamma-ray spectra from the Milky Way Halo**
- **Line searches:**
 - **no significant feature observed**
 - **constraints are up to 2 orders of magnitude stronger than those obtained in the previous Fermi-LAT analysis in 2015**
 - **The improvement is due to:**
 - **Combined-likelihood analysis technique**
 - **More accurate modeling of the astrophysical background between 1 and 10 GeV**
 - **Larger data statistics**
- **We also implemented a box-like feature search, testing the low-mass mediator scenarios and finding no globally significant features**